



Semnan University



Investigation on Turbulent Nanofluid Flow in Helical Tube in Tube Heat Exchangers

Puriya Mohamad Gholy Nejad, Ali Reza Solaimany Nazar*, Zohreh Rahimi-Ahar, Hajar Rajati

Department of Chemical Engineering, University of Isfahan, Isfahan, Iran

PAPER INFO

Paper history:

Received: 2017-11-04

Received: 2018-08-12

Accepted: 2018-08-18

Keywords:

Nanofluids;
Coiled double tubes heat exchanger;
Friction factor;
Heat transfer coefficient.

ABSTRACT

In this study, the thermal characteristics of turbulent nanofluid flow in a helical tube in the tube heat exchanger (HTTHE) were assessed numerically through computational fluid dynamics (CFD) simulation. The findings of both the turbulent models: realizable k-epsilon ($k-\epsilon$) and re-normalisation group (RNG) k-epsilon were compared. The temperature distribution contours show that realizable and RNG k- ϵ models, together with the swirl dominated flow are of more uniform temperature distributions. The proper prediction of two layer theory leads to having a uniform temperature distribution and proper dimensionless wall distance (Y^+). The turbulent flow and heat transfer of two nanofluids (SiO_2 , Al_2O_3) and base fluid with respect to swirl dominated flow was simulated through the RNG model. The effects of the concentration of nanoparticles on heat transfer characteristics in HTTHE and two turbulent models were analyzed in a comprehensive manner. It is concluded that up to 1% concentration of SiO_2 and 1% concentration of Al_2O_3 , similar heat transfer characteristics are observed. Comparison between the CFD results with the predicted values for friction factor coefficient (f) and Nusselt number (Nu) calculated through experimental correlations indicate the maximum errors of 6.56% and 0.27%, respectively.

DOI: 10.22075/jhmtr.2018.12696.1191

© 2019 Published by Semnan University Press. All rights reserved.

1. Introduction

Numerous experimental and numerical assessments have been published to develop the better understanding of the nanofluids behavior [1], thermal characteristics in heat exchangers [2], their modelling [3] and CFD simulation [4]. The related literature review indicates that only a few studies are run on HTTHEs [5]. These heat exchangers create turbulence and promote swirl in convective heat transfer in the fluid and cause effective mixing of fluid and provide a large area. Helically tube exchanger is superior due to its physical configuration and generating secondary flow compared to the conventional tube heat exchangers. The secondary flow and increased heat transfer potential of nanofluids in the helically coiled tube heat exchangers is applied to increase the heat exchangers effectiveness; thus, a reduction of size in heat

exchangers [6]. Due to the growth of industrial applications regarding heat transfer with respect to the energy and environmental concerns, heat exchanger configurations have been improved to transfer heat in an efficient manner. Applying the fin and tube [7] or compact [8] heat exchanger, heat exchanger equipped with helical membrane coils [9] and improving the thermal conductivity of basefluid would enhance the convective heat transfer of these apparatuses. Investigators recommend improving the thermal conductivity of basefluid to enhance the performance of heat exchangers by applying nanofluids, which are a liquid–solid mixture of nanoparticles like metal, oxides, and some other compounds. Here, the basefluids usually consist of water, alcohols, and oils. Due to large surface areas of the nanoparticles, nanofluids obtain superior properties, in

*Corresponding Author: A. R. Solaimany Nazar, Department of Chemical Engineering, University of Isfahan, Isfahan, Iran
Email: asolaimany@eng.ui.ac.ir

high thermal conductivity, stability, and homogeneity [10].

The enhancement in thermal conductivity of nanofluids depends on temperature, particles volume fraction, material shape, type, and size. Vajjha and Das [11] assessed the dependency of thermal conductivity on both the temperature rises from 298 to 363 K and particle concentration up to 10 %. The results indicate that an increase in temperature and concentration of nanoparticles would lead to an increase in the thermal conductivity of nanofluids in comparison with the basefluids.

An experimental investigation was carried out by Hashemi and Akhavan-Behabadi [12] to assess the pressure drop and heat transfer characteristics of nanofluid flow inside a horizontal helical tube subjected to laminar flow regime and constant heat flux. The CuO nanoparticles were dispersed in an industrial oil with a concentration of 0.5–2 %. The effect of some parameters like fluid temperature, Reynolds number (Re) and nanofluid particle concentration on pressure drop of the flow and heat transfer coefficient, were investigated as well. Their results revealed that by using the helically coiled tube and the nanofluid instead of basefluid, the heat transfer performance improves. Narrein and Mohammed [6] performed a numerical assessment on the effects of different nanoparticle, with different diameters and volume concentrations in basefluid types of water, engine oil, and ethylene glycol, influencing the thermal and hydraulic characteristics in helically coiled tube heat exchanger subjected to laminar flow. Their results indicated that nanofluids would improve the thermal properties and performance of the exchanger, while this fact is accompanied by an increase in pressure drop. They concluded that the Nu is at its highest when CuO is being utilized.

The thermal performance of single and hybrid type nanofluid was assessed in a coiled heat exchanger at laminar flow operating conditions and constant wall temperature by Allahyar et al. [13]. The maximum heat transfer rate was achieved using a hybrid type at a concentration of 0.4 vol % which is 31.58 % higher than that of water.

The heat transfer characteristics of Al₂O₃-Cu/water hybrid nanofluid was investigated in a permeable channel by Mollaahmadi et al. [14]. The effects of the Re and the concentration of nanoparticles, on the heat transfer, were examined. The results showed that an increase in the Re increases the Nu. By using the hybrid nanofluid, rather than pure nanofluid, the heat-transfer coefficient increased significantly.

The effect of using Al and Cu nanofluids on the convective heat transfer inside a spiral coil was studied by Tajik Jamal-Abad et al. [15]. The results showed that the nanofluid significantly increases the convective heat transfer coefficient, and Cu-water nanofluid has more thermal characteristics than Al- water nanofluid.

From reviewing the previous literature, it is obvious that no sufficient attempts made to study the effects of

different turbulent models and different nanoparticles in HTTHEs under turbulent flow regime in both inner and annulus tube sides. In order to shade more light on this issue and pave the way in this field, an attempt was made to assess and examine a 3D turbulent flow with respect to the effects of different turbulent models and two introduced nanofluids. The objective of this article is to study the heat transfer behavior and pressure drop of water-based SiO₂ and Al₂O₃ subject to different turbulent models. It is expected that the findings here would fulfill the research gap regarding HTTHEs operating with nanofluids to a certain degree.

2. Methodology

2.1 Numerical model

A commercially CFD code was applied to run the numerical calculations of the subject 3D geometry. The computational geometry was developed in Gambit, and heat transfer and pressure drop analysis was done using Fluent. The considered heat exchanger geometry with di,i, di,o, R, and H dimentions was depicted in Fig. 1. The geometric parameters and inlet conditions of this heat exchanger are presented in Table 1. The cold nanofluid flows in the annulus tube side, while the hot nanofluid flows in the inner coiled tube. The material of the heat exchanger component was of copper. Its physical properties are tabulated in Table 2. According to the obtained result by Rea et al. [16], the single-phase model is applied frequently for nanofluids thermal behavior prediction.

2.2 Governing equations

Setting the governing equations to complete the CFD analysis of the HTTHE is of major importance. In this study, the RNG k-ε turbulent model with enhanced wall treatment and swirl dominated flow, the RNG turbulent model with enhanced wall treatment without swirl dominated flow and the realizable k-ε model were selected. The mentioned equations are written as:

$$\nabla \cdot (\rho_{eff} U) = 0 \quad (1)$$

Table 1. Geometry and inlet conditions of CTITHE

	Inner tube	Outer tube
Outer diameter, m	0.00635	0.01587
Inner diameter, m	0.00475	0.01407
Coil diameter, m	0.3	0.3
Pitch, m	0.03174	0.03174
Number of turns	1.5	1.5
Tube material	Copper	Copper
Flow rate, LPM	2	10
Inlet temperature, °C	50	20

Table 2. Physical properties of copper

Density (kg/m ³)	Specific heat (J/kg.K)	Thermal conductivity (W/m.K)
9878	381	387.6

Momentum equation:

$$\nabla \cdot (\rho_{eff} \mathbf{U}\mathbf{U}) + \nabla P - \nabla \cdot (\boldsymbol{\tau} + \boldsymbol{\tau}^T) = 0 \quad (2)$$

Energy equation:

$$\nabla \cdot (\rho_{eff} c_{p,eff} \overline{T\mathbf{U}}) - \nabla \cdot (k_{eff} (\nabla \overline{T})) + (\overline{U'T'}) = 0 \quad (3)$$

The k-ε RNG turbulent model is applied as follows:

$$\nabla \cdot (\rho_{eff} k \mathbf{U}) = \nabla \cdot [(\mu_{eff} + \frac{\mu_t}{\sigma_k})(\nabla k)] + G_k - \rho_{eff} \varepsilon, \quad (4)$$

$$\nabla \cdot (\rho_{eff} \varepsilon \mathbf{U}) = \nabla \cdot [(\mu_{eff} + \frac{\mu_t}{\sigma_\varepsilon})(\nabla \varepsilon)] + C_{1\varepsilon} \frac{\varepsilon}{k} G_k - C_{2\varepsilon} \rho_{eff} \frac{\varepsilon^2}{k}$$

$$G_k = -\rho_{eff} \overline{U_i U_j} (\nabla U),$$

$$\mu_t = \rho_{eff} C_\mu \frac{k^2}{\varepsilon}$$

In the case of RNG model with swirl dominated flow, the swirl factor =0.07.

2.3 Grid testing and model validation

2.3.1 Grid testing

The 3D geometry of this heat exchanger with meshing is displayed in Fig. 2. A grid independence check was run to evaluate the effects of different grid size on the obtained outcomes. The grid independence was checked through four sets of hexahedral meshes of 325200, 461000, 688000, and 753200 cells, respectively. The last two types of mesh yielded similar results with respect to heat transfer coefficient and satisfactory Y+. In this study, by considering the accuracy of obtained results (temperature distribution and Y+) and in order to decrease the computational time, the set of 688000 cells were chosen.

2.3.2 Validation

The validation was made based on boundary conditions and geometry, introduced by Aly [5]. For validation purpose, the realizable k-ε turbulent model was used. The code was validated by comparing the flow results with the experimental correlations introduced by Gnielinski [17], Mishra and Gupta [18] and Ito [19]. The obtained CFD results were compared with the available experimental correlations presented in Table 3. It is observed that the obtained results show close agreement with Eqs. (5) through(7).

2.4 Numerical procedures

The numerical computations were run by solving the Eqs. (1-4), by applying the finite volume formulations. The numerical solution procedure adopts the SIMPLEC algorithm for pressure velocity coupling. The second-order upwind scheme was applied for momentum, turbulent kinetic energy- dissipation rate, and third-order QUICK discretization scheme was applied for energy

equation. The considered solutions converged when the normalized residual value ≤10⁻¹² for energy balance and ≤10⁻¹¹ for continuity, velocity, k, and ε.

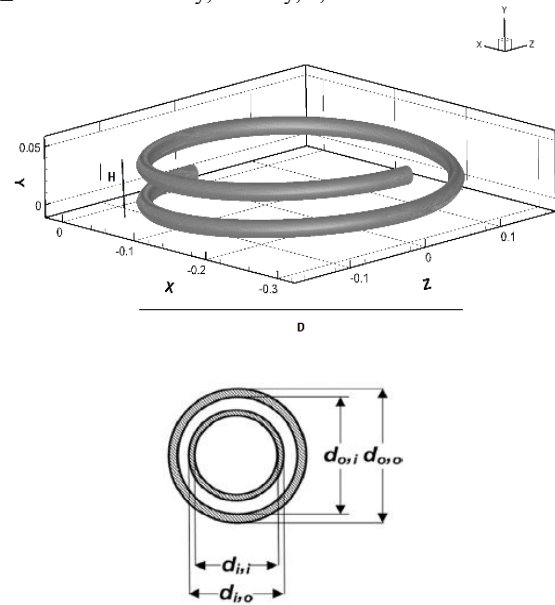


Figure 1. Schematic diagram and cross section of CTITHE

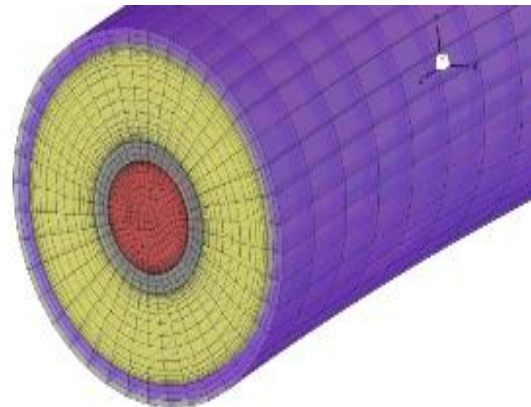


Figure 2. Grid system for CTITHE

Table 3. Friction factor and Nusselt number correlations

Author	Correlation	condition	Eq.
Gnielinski [17]	$Nu = \frac{Pr \cdot Re(f/8)}{1.0 + 12.7 \sqrt{f/8} (Pr^{2/3} - 1)}$ $f = 0.3164 Re^{-0.25} + 0.03 \delta^{0.5}$	$Re > 2.2 \times 10^4$	(5)
Mishra Gupta [18]	$f = f_s + 0.03 \delta^{0.5}$ $f_s = 0.3164 Re^{-0.25}$	$4500 < Re < 10^5$	(6)
Ito [19]	$f = 0.304 Re^{-0.25} + 0.029 \delta^{0.5}$	$300 > Re \delta^2 > 0.034$	(7)

Table 4. Thermophysical properties of the base fluid and the nanoparticles [20, 21].

Property	Water	Al ₂ O ₃	SiO ₂
Density (kg/m ³)	998.2	3300	2200
Specific heat (J/kg.K)	4182	880	703
Thermal conductivity(W/m.K)	0.6	42.34	1.2
Dynamic viscosity	0.001003	-	-

In order to represent the results, the following dimensionless parameters are introduced:

$$\text{Re} = \frac{\rho U d_h}{\mu}, \text{Pr} = \frac{C_p \mu}{K} \quad (8)$$

$$\text{Nu} = \frac{h d_h}{K}$$

Dean number (Dn), which represents the magnitude of secondary flow is presented as:

$$\delta = \frac{d_h}{D_c}, \text{Dn} = \text{Re} \delta^{1/2} \quad (9)$$

The heat transfer coefficient (h) of water is defined as follows:

$$h = \frac{q}{(T_w - T_b)} \quad (10)$$

$$q = \frac{\dot{m} C_p (T_i - T_o)}{\pi d_h L}$$

The friction factor, f, is determined as:

$$f = \frac{2 \Delta p d_h}{\rho U^2 L} \quad (11)$$

2.5 Thermophysical Properties of Nanofluids

In order to conduct the numerical simulation for nanofluids, the thermophysical properties of nanofluids were determined. In this study, the nanoparticles were of Al_2O_3 and SiO_2 type. The thermophysical properties of the basefluid and the nanoparticles involved here are presented in Table 4. The aim was to deepen the effect of using nanofluids with different amounts of thermal conductivity on heat transfer enhancement in heat exchangers.

The density of nanofluid, ρ_{nf} is obtained from the following equation [5]:

$$\rho_{nf} = (1 - \phi) \rho_f + \phi \rho_{np} \quad (12)$$

The effective heat capacity is calculated through the following equation [5]:

$$(\rho C_p)_{nf} = (1 - \phi) (\rho C_p)_f + \phi (\rho C_p)_{np} \quad (13)$$

The effective thermal conductivity is obtained through the following correlation [5]:

$$k_{eff} = k_{static} + k_{Brownian} \quad (14)$$

$$k_{static} = k_f \left[\frac{-2\phi(k_f - k_{np}) + (k_{np} + 2k_f)}{\phi(k_f - k_{np}) + (k_{np} + 2k_f)} \right] \quad (15)$$

$$k_{Brownian} = 5 \times 10^4 \beta \phi \rho_f C_{pf} \sqrt{\frac{KT}{2}} f(T, \phi) \quad (16)$$

where $K = 1.3807 \times 10^{-23}$ J/K.

The modified $f(T, \phi)$ function is obtained as follows:

$$f(T, \phi) = (3.917 \times 10^{-3} + 2.8217 \times 10^{-2} \phi) \left(\frac{T}{273.15} \right) + (-3.0669 \times 10^{-2} \phi - 3.91123 \times 10^{-3}) \quad (17)$$

The effective viscosity is obtained through the following mean empirical correlation [11]:

$$\mu_{eff} = \mu_f \times \left(\frac{1}{1 - 34.87 \left(\frac{d_p}{d_f} \right)^{-0.3} \times \phi^{1.03}} \right) \quad (18)$$

$$d_f = \left[\frac{6M}{N \pi \rho_{f0}} \right]^{1/3} \quad (19)$$

where $N = 6.022 \times 10^{23} \text{ mol}^{-1}$.

The average absolute relative error (AARE, %) for all the given data points at different Re is calculated by the following equation:

$$\text{AARE}(\%) = \frac{100}{N} \sum_{i=1}^N \left| \frac{X_i^{CFD} - X_i^{ref}}{X_i^{ref}} \right| \quad (20)$$

where, X_i^{CFD} and X_i^{ref} are the Nu or f calculated by CFD and predicted by the model from references, respectively. N is the number of available data points at different Re.

2.6 Boundary conditions

Boundary conditions in the model are summarized as follow:

- Inner tube side mass flow rate: 2-5 LPM and annulus tube side mass flow rate: 10-25 LPM
- Inner tube side nanofluid temperature: 50°C and annulus tube side nanofluid temperature: 20°C
- Pressure outlet in both tube sides: 1 bar
- No-slip boundary condition on the walls
- Adiabatic wall boundary condition on the outer wall
- The coupled temperature on the interface wall

3. Results and discussion

In this study, the selected nanoparticles were promising for heat transfer applications owing to their excellent specific heat and thermal conductivities as well as lower viscosities even at high concentrations, good dispersibility [22], higher effectiveness in the case of considering nanoparticle price [23].

The heat transfer characteristics of nanofluids were compared based on Re. SiO_2 nanofluid was attributed to the Brownian particle motion; therefore, a further increase for the heat transfer capability of SiO_2 nanoparticles. SiO_2 nanoparticles present a large surface area which enhances the heat transfer characteristics of the nanofluid.

The presenting of the Nu as a function of the Re indicates enhancement in the convection heat transfer. Typically, the nanofluids obtain higher Nu than water with an equal Re. The well-known correlation of Dittus-Boelter confirms that an increase in Re leads to increase in Nu and hence, the heat transfer coefficient of nanofluid [24]. The comparison of the Nu of SiO_2 nanofluid with that of Al_2O_3 nanofluid result obtained by Aly [5] in the inner and annulus tube sides of the HTHE are presented in Fig. 3 (a) and (b), respectively. The Nu from Fig. 3 was compared when subjected to the same Re in 11600 to 28120 ranges. The numerical results indicated that due to the low thermal conductivity of SiO_2 nanofluid, Nu is

higher than that of other nanofluids. An increase in Re leads to increase in Nu . The calculated AARE % of Nu_i and Nu_o in this study in relation to Gnielinski's correlation are 1.4 % and 3.6 %, respectively. The obtained results revealed the good agreement between the computational model and the experimental correlation, which in fact confirms the accuracy of this model.

The friction factors calculated from the CFD results regarding pressure drop and the variant friction factors with respect to Re for SiO_2 nanofluid and their comparison with water and the results reported by Mishra and Gupta and Ito are presented in Fig. 4. According to Blasius equation and Eq. (6), an increase in Re leads to a reduction in the calculated f [25]. This fact is confirmed through this study, which f decreases when Re increases (see Fig. 4). It is also expected from the particles Brownian movement by adding nano particle to the water, which causes an increase in the momentum transfer, the obtained f for nanofluid is more than water. It should be noted that according to Fig. 4, the Ito's model shows less f than Mishra and Gupta's model subjected to the same Re . Consequently, Ito's equation is not a proper correlation for predicting the nanofluid pressure drop in this study.

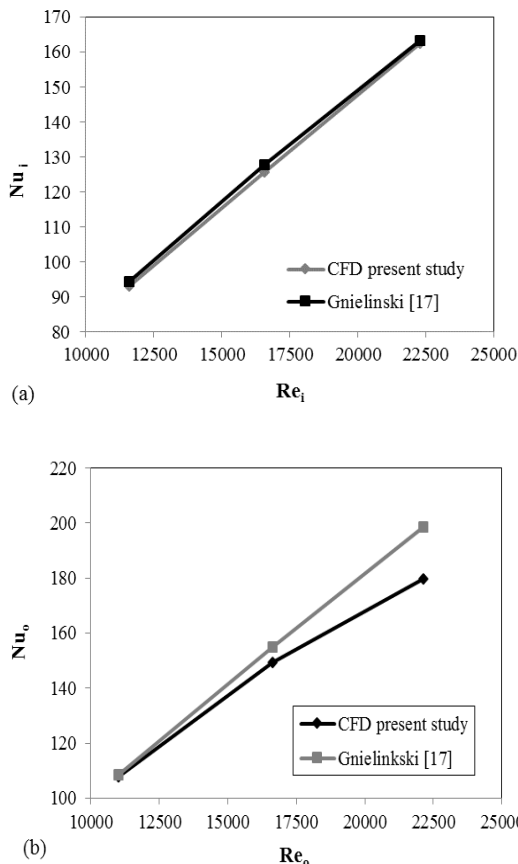


Figure 3. Comparison of Nu between the present study and Gnielinski [17] based on Re (a) inner tube side, (b) annulus tube side.

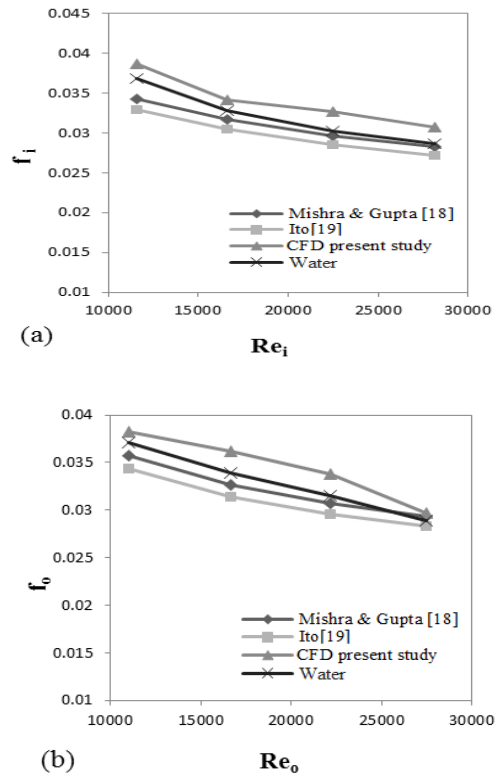


Figure 4. f versus Re (a) inner tube side, (b) annulus tube side

The heat transfer coefficient versus Re for HTTHE is shown in Fig. 5 (a) and (b) for the inner and the annulus tube sides, respectively. With an increase in Re , the importance of thermal conductivity in heat transfer enhancement becomes less considerable [26]. It is observed from Fig. 5 that the highest heat transfer coefficient is obtained for SiO_2 and Al_2O_3 nanofluids. At 1% volume concentration of SiO_2 nanofluid and Al_2O_3 nanofluid, the heat transfer coefficient of both the nanofluids is 8.6 % and 8.2 % greater than the basefluid in annulus tube side, respectively; while this value is 4.3 % and 1.5 % in inner tube side. This behavior is probably due to the wall effect, which leads to the turbulent flow. Due to an increase in heat transfer coefficient by using SiO_2 and Al_2O_3 and therefore an improvement in the heat transfer characteristics in both the nanofluids, these nanofluids were recommended to be used in heat exchangers. The possible explanation behind this phenomena is the fact that at 1% concentration of SiO_2 and 1% concentration of Al_2O_3 , these two nanofluids show similar behavior.

The simulated Nu versus the predicted Nu of Eq. (5) and f of Eq. (6) are presented in Figs. 6 (a) and (b), respectively. In this figure, the values of predicted Nu and f are in accordance with the simulated ones in this study. Here, the maximum error of Nu is 6.56 %, and the same amount for f is 0.27 %. It is deduced that Eq. (6) is valid for the tested nanofluids in the turbulent flow regime. In this study, it is found that nanofluids behave as a homogeneous fluid. The findings of this assessment

indicate similar trends of increase in f with respect to an increase in Re , a similar finding by El-Maghlany et al. [27].

Temperature distribution contours for three different models for inner and annulus tube sides are shown in Figs. 7 and 8, respectively. Here, it is observed that the RNG model could predict the nanofluid behavior in temperature distribution contours in a proper manner, provided that the swirl dominated flow is considered in the equations. As observed in Figs. 7 and 8 the RNG model shows the similar result with the realizable $k-\epsilon$ model when the swirl dominated flow is applied; thus, the RNG model is adopted in evaluating the heat transfer characteristics of nanofluid in HTTHE. These contours show that realizable $k-\epsilon$ and RNG $k-\epsilon$ models, together with the swirl dominated flow are of more uniform temperature distribution. Temperature differences in Figs. 7 (a), (b) and (c) are 3.9, 3.7 and 12.6 for inner tube side and the same at Figs. 8 (a), (b) and (c) are 5, 3.7 and 9.3 for annulus tube side, respectively. Thus the RNG model, together with the swirl dominated flow shows more uniform temperature distribution at any cross section than the other two models. In a previous study [9], it was reported that realizable $k-\epsilon$ model is more precise than the RNG turbulent model, while, according to the obtained results in this study (Figs. 7 and 8), the RNG model could predict the nanofluid behavior in temperature distribution contours better than realizable $k-\epsilon$ model, provided that the swirl dominated flow is considered.

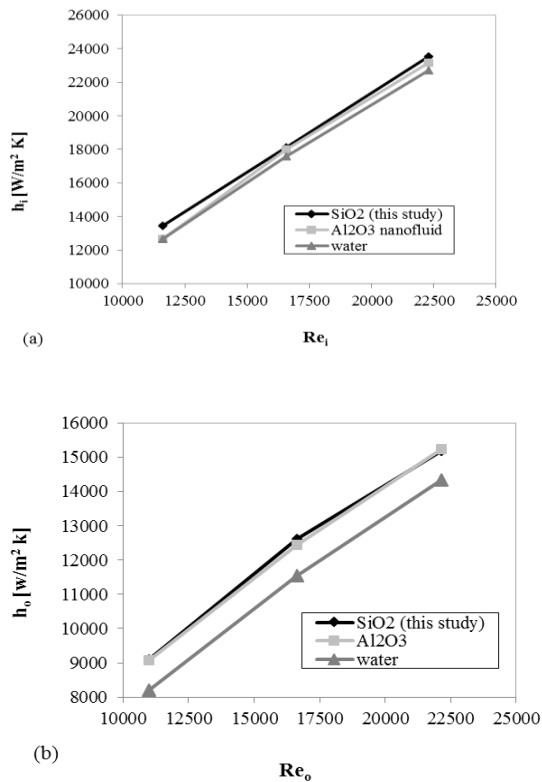


Figure 5. Heat transfer coefficient versus Re (a) inner tube side, (b) annulus tube side

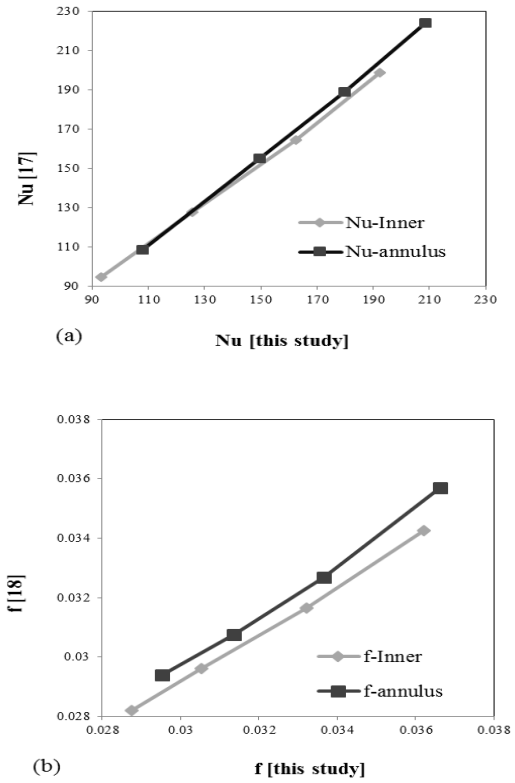


Figure 6. Comparison of the simulated values of (a) Nu , (b) f , with those predicted by Gnielinski [17] and Mishra and Gupta [18], respectively

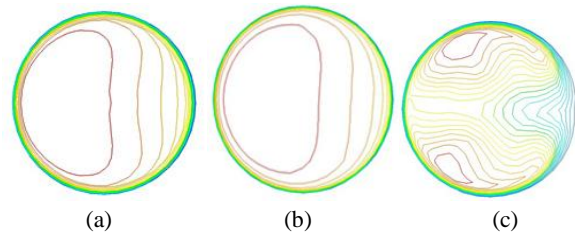


Figure 7. Comparison of temperature distribution contours among (a) realizable, (b) RNG, (c) RNG where no dominated flow model for inner side of the tube is of concern.

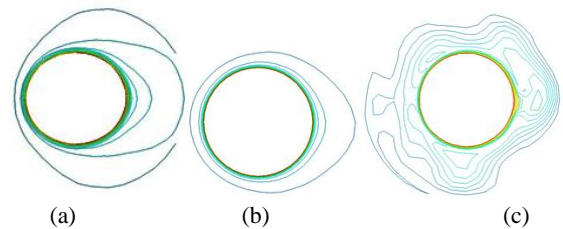


Figure 8. Comparison of temperature distribution contours among (a) realizable, (b) RNG, (c) RNG where no dominated flow model for outer side of tube is of concern.

The temperature vector in HTTHE for RNG model where the swirl dominated flow is of concern and the three different 325200, 461000, and 688000 cells are shown in Fig. 9. As observed here, as the mesh size increases, the

temperature profile for nanofluid is more vivid. As for the vectors in this figure, the laminar flow is evident near the wall, and the turbulent flow is evident in the center parts of the tube. This normal behavior is clearly observed in 688000 cells, where small temperature range due to the systematic establishment of the boundary layers is observed as well. This phenomenon improves the convective heat transfer coefficients on the boundaries where a considerable enhancement of heat transfer is achieved. It is deduced that when the mesh size decreases, the value of Y^+ decreases; as for 688000 cells, the value of Y^+ is almost 1. According to the result obtained by Aly [5], the proper value for Y^+ is 1. Thus it is deduced that the value obtained here by 688000 cells is an appropriate value for simulation due to the proper value of Y^+ and clear temperature profile.

4. Conclusion

In this article, the characteristics of pressure drop and convective heat transfer of SiO_2 nanofluid flowing in HTTHE is assessed. The following conclusions can be expressed according to obtained results:

- The 3D k- ϵ RNG model with and without swirl dominated flow, and realizable k- ϵ turbulence model were assessed. Due to uniform temperature distribution, adopting the two layers theory and proper Y^+ , the RNG k- ϵ model with the swirl dominated flow is proper to simulate the turbulent flow in HTTHE.
- The changes in f and Nu against Re for SiO_2 and Al_2O_3 nanofluids at 1 % concentration was also assessed. The results obtained from the simulation of Al_2O_3 indicate a good agreement with that of reported in the related literature. The heat transfer coefficient for SiO_2 and Al_2O_3 nanofluids at 1 % concentration in a separate manner demonstrated a better result than that of water.
- Comparison between the CFD study against predicted values for f and Nu through experimental correlations indicate that experimental correlations are established based on single phase fluid data which holds true for multiphase flow with maximum errors less than 6.56 %.

Nomenclature

C_p	Specific heat at constant pressure, J/kg.K
C	Model parameter
D	Coil diameter, m
Dn	Dean Number
d	Tube diameter, m
f	Darcy-Weisbach friction factor
h	Heat transfer coefficient
H	Coil pitch, m
k	Turbulent kinetic energy, m^2/s^2
L	Length of the tube, m
M	Molecular weight of the basefluid, g/gmol
\dot{m}	Mass flow rate, kg/s
K	Thermal conductivity, W/m.K
Nu	Nusselt number
P	Pressure, Pa
Pr	Prandtl number

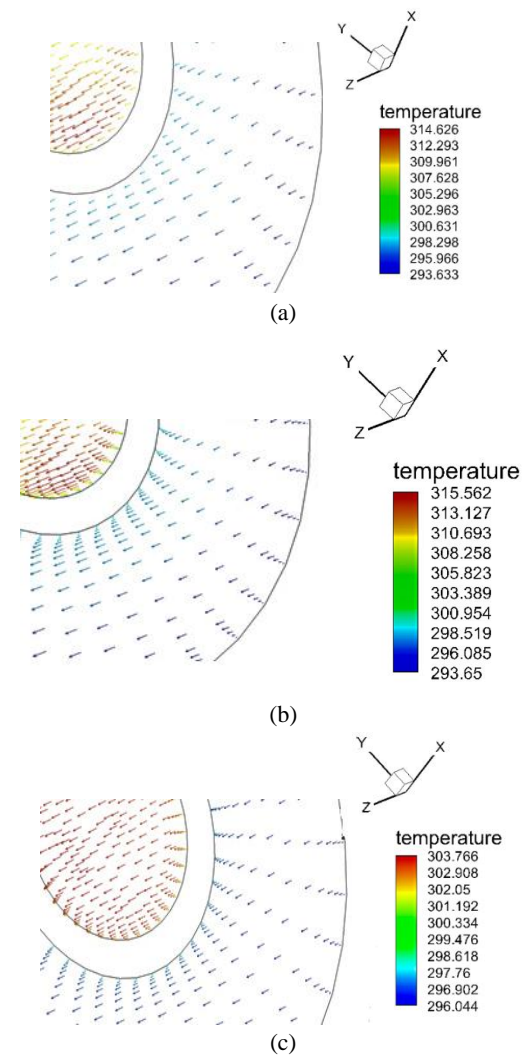


Figure 9. Temperature profile vectors in CTITHE (a) 325200, (b) 461000 and (c) 688000 grid cells

q	Heat flux, W/m ²
Q_c	Cold water flow rate, LPM
Q_h	Hot water flow rate, LPM
R	Coil radius, m
Re	Reynolds Number
T	Temperature, K
U	Velocity component in the flow direction, m/s
U'	Root-mean-square turbulent velocity fluctuation, m/s
Y^+	Dimensionless distance from the wall, $u_{\tau}y/m$

Greek symbols

B	Curve-fit relations
δ	Curvature ratio
δ_{ij}	Dirac delta function
ϵ	Turbulent dissipation rate, m^2/s^3
ρ	Density of test fluid, kg/m ³
μ	Dynamic viscosity, kg/m.s
σ_{τ}	Turbulent Prandtl number in the energy equation
σ_k	Diffusion Prandtl number for k
Δ	Difference operator
ϕ	Nanoparticle volume concentration

Subscript

b	Bulk quantity
bf	Basefluid
c	Cold
eff	Effective
f	Fluid
h	Hot
i,j,k	General spatial indices
i	Inner or inlet
nf	Nanofluid
o	Outlet or outer
P	Nanoparticle
w	Wall condition

References

- [1] P. J. Fule, B. A. Bhanvase, S. H. Sonawane, Experimental investigation of heat transfer enhancement in helical coil heat exchangers using water based CuO nanofluid. *Advanced Powder Technology*, 28(9) 2288-2294, (2017).
- [2] A. Shahsavar, Z. Rahimi, M. Bahiraei, Optimization of irreversibility and thermal characteristics of a mini heat exchanger operated with a new hybrid nanofluid containing carbon nanotubes decorated with magnetic nanoparticles, *Energy Conversion and Management*, 150, 37-47, (2017).
- [3] M. Zeeshan, S. Nath, D. Bhanja, Numerical study to predict optimal configuration of fin and tube compact heat exchanger with various tube shapes and spatial arrangements, *Energy Conversion and Management*, 148, 737-752, (2017).
- [4] R. S. Dondapati, V. Saini, K. N. Verma, P. R. Usurumarti, Computational prediction of pressure drop and heat transfer with cryogen based nanofluids to be used in micro-heat exchangers, *International Journal of Mechanic Science*, 130, 133-142, (2017).
- [5] W. I. A. Aly, Numerical study on turbulent heat transfer and pressure drop of nanofluid in coiled tube-in-tube heat exchangers. *Energy Conversion and Management*, 79, 304-316, (2014).
- [6] K. Narrein, H. A. Mohammed, Influence of nanofluids and rotation on helically coiled tube heat exchanger performance, *Thermochimica Acta*, 564, 13-23, (2013).
- [7] P. Pongsoi, S. Pikulkajorn, S. Wongwises, Effect of fin pitches on the optimum heat transfer performance of crimped spiral fin-and-tube heat exchangers, *International Journal of Heat and Mass Transfer*, 55(23), 6555-6566, (2012).
- [8] D. R. Ray, D. K. Das, R. S. Vajjha, Experimental and numerical investigations of nanofluids performance in a compact minichannel plate heat exchanger, *International Journal of Heat and Mass Transfer*, 71, 732-746, (2014).
- [9] Z. Zhao, D. Che, Influence of tube arrangement on the thermal hydraulic performance of a membrane helical-coil heat exchanger, *Numerical Heat Transfer, Part A: Applications*, 62(7), 565-588, (2012).
- [10] N. K. Gupta, A. K. Tiwari, S. K. Ghosh, Heat transfer mechanisms in heat pipes using nanofluids – A review. *Experimental Thermal Fluid Science*, 90, 84-100, (2018).
- [11] R. S. Vajjha, D. K. Das, Experimental determination of thermal conductivity of three nanofluids and development of new correlations, *International Journal of Heat and Mass Transfer*, 52(21), 4675-4682, (2009).
- [12] S. M. Hashemi, M. Akhavan-Behabadi, An empirical study on heat transfer and pressure drop characteristics of CuO–base oil nanofluid flow in a horizontal helically coiled tube under constant heat flux, *International Communications in Heat and Mass Transfer*, 39, 144-151, (2012).
- [13] H. R. Allahyar, F. Hormozi, B. ZareNezhad, Experimental investigation on the thermal performance of a coiled heat exchanger using a new hybrid nanofluid, *Experimental Thermal and Fluid Science*, 76, 324-329, (2016).
- [14] M. Moahammadi, M. Hemmat Esfe, Buoyancy driven heat transfer of a nanofluid in a differentially heated square cavity under effect of an adiabatic square baffle, *Journal of Heat and Mass Transfer Research*, 1, 1-13, (2015).
- [15] A. Z. M. Tajik Jamal-Abad, M. Dehghan, Analysis of variance of nano fluid heat transfer data for forced convection in horizontal spirally coiled tubes, *Journal of Heat and Mass Transfer Research*, 2, 45-50, (2015).
- [16] U. Rea, T. McKrell, L.W. Hu, J. Buongiorno, Laminar convective heat transfer and viscous pressure loss of alumina–water and zirconia–water nanofluids, *International Journal of Heat and Mass Transfer*, 52(7), 2042-2048, (2009).
- [17] V. Gnielinski, Heat transfer and pressure drop in helically coiled tubes, *Proceedings 8th International Heat Transfer Conference*, San Francisco, Hemisphere, Washington DC, 6, 2847-2854, (1986).
- [18] P. Mishra, S. N. Gupta, Momentum transfer in curved pipes. 2. Non-Newtonian fluids. *Industrial & Engineering Chemistry Process Design and Development*, 18(1), 137-142, (1979).

- [19]H. Ito, Friction factors for turbulent flow in curved pipes, *Journal of Basic Engineering*, 81(2), 123-134, (1959).
- [20]H. Yarmand, S. Gharekhani, S. N. Kazi, E. Sadeghinezhad, M.R. Safaei, Numerical investigation of heat transfer enhancement in a rectangular heated pipe for turbulent nanofluid, *The Scientific World Journal*, Article ID 369593, 2014, 1-9, (2014).
- [21]V. Bianco, F. Chiacchio, O. Manca, S. Nardini, Numerical investigation of nanofluids forced convection in circular tubes, *Applied Thermal Engineering*, 29(17), 3632-3642, (2009).
- [22]A. Kumar, A. Kumar, A. Rai, Characterization of TiO₂, Al₂O₃ and SiO₂ Nanoparticle based Cutting Fluids, *Material Today Proceedings*, 3(6), 1890-1898, (2016).
- [23]Z. Hajabdollahi, H. Hajabdollahi, P. F. Fu, The effect of using different types of nanoparticles on optimal design of fin and tube heat exchanger, *Asia Pacific Journal of Chemical Engineering*, 1-14, (2017).
- [24] K. S. Mikkola, V. Puupponen, S. Granbohm, H. A. Ala-Nissila, T. Seppälä, Influence of particle properties on convective heat transfer of nanofluids, *International Journal of Thermal Science*, 3, 101-114, (2016).
- [25]H. Blasius, The boundary layers in fluids with little friction, *Zeitschrift fuer Mathematik und Physik*, 56(1), 1-37, (1950).
- [26]D. Wen, Y. Ding, Experimental investigation into convective heat transfer of nanofluids at the entrance region under laminar flow conditions, *International Journal of Heat and Mass transfer*, 47(24), 5181-5188, (2004).
- [27] W. M. El-Maghlany, A.A. Hanafy, A.A. Hassan, M.A. El-Magid, Experimental study of Cu-water nanofluid heat transfer and pressure drop in a horizontal double-tube heat exchanger, *Experimental Thermal and Fluid Science*, 78, 100-111, (2016).